doi.org/10.36721/PJPS.2026.39.11.301.1

The influence of LINC00511 and MDM2/MDM4 in lung carcinoma: Implications for immunological therapeutic strategies

Fengyun Zhang[1] and Qiuwen Li[2]*

[1]Department of Internal Medicine, North China Electric Power University Hospital, Beijing, 102206, China
[2]Department of Medical Oncology, The Fourth Medical Center of the PLA General Hospital, Beijing, 100048, China

Abstract: **Background**: Immunotherapy has significantly improved the treatment of lung cancer, but some patients experience aggressive disease, the mechanisms of which remain unclear. In particular, the interaction between lncRNA and the MDM2/MDM4 pathway warrants in-depth exploration. **Objectives**: This study aimed to investigate the role of LINC00511 in promoting aggressive disease during immunotherapy for lung carcinoma by modulating MDM2/MDM4 expression. **Methods**: This study collected tissues from 30 lung cancer patients undergoing immunotherapy and used A549 cell lines. RT-PCR detected expression of LINC00511, while immunohistochemistry and immunofluorescence detected MDM2/MDM4 expression. Bioinformatics analysis and luciferase reporter assays were performed to confirm their relationship. Cell migration, invasion, proliferation and response to PD-1 inhibitors were assessed. **Results**: using A549 cells and female BALB/c nude mice (n=6 per group). LINC00511 was significantly upregulated in aggressive disease tissues and positively correlated with tumor stage. MDM2/MDM4 expression was also elevated ($P < 0.01$). LINC00511 directly targeted MDM2/MDM4. Silencing LINC00511 effectively inhibited tumor cell proliferation, migration, invasion and Ki-67 expression in vitro and in *vivo* . In the xenograft model, BALB/c nude mice treated with Nivolumab (0.1 mg/kg i.p. every 3 days) showed reduced tumor volume (mean ± SD: 445.6 ± 45.3 mm^3 vs. 720.4 ± 80.2 mm^3 in controls; $P < 0.01$).**Conclusion**: LINC00511 promotes hyperprogressive disease in lung cancer during immunotherapy by upregulating MDM2/MDM4. Inhibition of LINC00511 effectively reverses tumor progression, suggesting a potential therapeutic target.

Keywords: Aggressive disease; LINC00511; Lung carcinoma; MDM2/MDM4

Submitted on 29-11-2024 – Revised on 27-02-2026 – Accepted on 18-03-2026

INTRODUCTION

Lung carcinoma is a highly prevalent solid tumor with significant morbidity and mortality (Siegel *et al*., 2025). The five-year survival rate remains low. Although diagnostic methods and treatment strategies have been developed, mortality remains stubbornly high (Reck *et al*., 2024). Significant progress has been made in immunotherapy for various solid tumors. The phenomenon of pseudoprogression—a condition in which tumors initially appear to grow on imaging scans (e.g., after radiation or immunotherapy) but are not truly progressing—may occur in some patients with lung carcinoma, leading to the development of the Immune-related Response Evaluation Criteria in Solid Tumors (iRECIST) criteria for evaluating immunotherapy efficacy (Ippolito *et al*., 2021). These criteria can be used to assess the efficacy of immunotherapy. Some patients, however, experience aggressive disease (AD), characterized by accelerated tumor growth after immunotherapy (Rodrigo *et al*., 2024). LncRNAs can act as oncogenes by inhibiting tumor suppressor genes, including by repressing endogenous cancer suppressors (Kai-Xin *et al*., 2021). For example, certain lncRNAs can promote lung cancer progression as oncogenes, such as under the induction of transcription factor SP1 via the LINC00127/FOXD1 axis (Abdi *et al*., 2023). LINC00511 could play a crucial role in regulating cell signaling transduction. The circ_0079586/LINC00511 axis regulates cell proliferation, apoptosis, migration and metastasis. LINC00511 promotes tumor proliferation by targeting the miR-625-5p/NFIX axis, making it a potential therapeutic target (Wu *et al*., 2024). LINC00511 promotes the occurrence and progression of liver cancer by inducing miR-195. So it could be adopted as a potential biomarker for predicting the occurrence of liver carcinoma (Zhang et al., 2022; Hu *et al*., 2020). In non-small cell lung cancer (NSCLC), LINC00511 promotes tumor progression by binding to EZH2 (Enhancer of zeste homolog 2) and lysine-specific demethylase 1 (LSD1), thereby downregulating LATS2 and KLF2 (Liu *et al*., 2022).

The MDM family plays a crucial role in normal epithelial development (Gao *et al*., 2026). This regulatory function is crucial for maintaining cellular integrity. The MDM family is notably characterized by its negative regulation of the tumor suppressor p53, thereby modulating cellular stress responses. The abnormal increase in MDM family protein expression was closely associated with increased tumor incidence (Liu *et al*., 2024). The most notable feature of the MDM family is its negative regulation of the tumor suppressor p53, thereby modulating cellular stress responses. Dysregulation and overexpression of MDM2/MDM4 are closely associated with increased

**Corresponding author:* e-mail: zhanzhuikeng7sr@126.com

tumor incidence and recurrence risk (Koelsche *et al*., 2021). Immune checkpoint inhibitors can enhance IFN-γ expression by modulating the tumor microenvironment and activating IRF-8. This cascade reaction is significantly correlated with tumor progression. The AD could be caused if there was amplification of MDM2. At present, a phase I study on MDM2 is underway to prevent AD caused by immunological therapy (Nuñez et al., 2023; Zhang *et al*., 2021).

Justification of animal model: BALB/c nude mice are widely used for xenograft studies due to their tolerance of human tumor cells. However, they lack mature T cells and therefore cannot fully recapitulate PD-1/PD-L1 blockade mechanisms.This model was used to isolate the cell-autonomous effects of LINC00511 on tumor growth independent of adaptive immunity; findings require validation in immunocompetent models.

This study aims to investigate the mechanism by which LINC00511 promotes aggressive disease during lung cancer immunotherapy via the MDM2/MDM4 pathway. A biomarker for predicting patients with aggressive disease could be screened for. The theoretical basis for the clinical diagnosis and treatment on lung carcinoma could be provided. The signal pathway mechanism is shown in figure 1.

MATERIALS AND METHODS

Tissue and cell culture

All tissue samples were obtained with written informed consent from the patients and the Ethics Committee of Ethics Committee of the Fourth Medical Center of the PLA General Hospital approved the study protocol**.** Among the 30 lung cancer cases (n = 30), 18 were diagnosed as lung adenocarcinoma, 10 as squamous cell carcinoma and 2 as large cell carcinoma, based on histopathological evaluation. The cohort included 17 male and 13 female patients. The average age was 63.4 ± 5.8. The clinical information of these patients was complete. Inclusion criteria for patient tissue samples were histologically confirmed lung carcinoma and completion of at least two cycles of immunotherapy. Exclusion criteria included prior malignancy, active autoimmune disease, or incomplete clinical records.

The human lung carcinoma cell strain A549 was purchased from the ATCC Center in the USA. Cells were cultured in RPMI1640 medium (Sigma-Aldrich, USA) supplemented with 10% fetal bovine serum (FBS). Prior to experiments, cells were serum-starved for 24 hours.

Luciferase reporter gene assay

The binding site between LINC00511 and MDM2/MDM4 was predicted using TargetScan. The pGL13 vector containing the LINC00511 sequence was synthesized. The cells were transfected with miR-NC or the LINC00511 inhibitor. Luciferase activity was measured using a commercial kit (Promega, Cat# E1910). Each independent experiment was performed in triplicate wells per condition and the experiment was repeated three times (n = 3 per group). The experimental unit was one well.

Cell transfection

shLINC00511, shNC, LINC00511 mimic and LINC00511 inhibitor were synthesized by Suzhou Jima Biological Co., Ltd. Referring to the methods in previous literature (Deng *et al*., 2018), the A549 cells were transfected with Lipofectamine 2000 (Shanghai Thermo Fisher Technology Co., LTD) according to the specifications when the cellular concentration was up to sixty percent to seventy percent. Cells were harvested for downstream assays (RNA extraction, protein lysis, or functional assays) at 48 hours post-transfection, unless otherwise specified. A non-targeting shRNA sequence (shNC) and an equal volume of PBS served as negative controls for shLINC00511 and drug administration, respectively. Each transfection condition was performed in triplicate wells and the experiment was repeated three times. The experimental unit was one well.

Immunohistochemistry staining

The tissue was dehydrated and fixed. They were cut into pieces. 4-HNE expression was assessed to evaluate oxidative stress. Inflammatory cell markers were analyzed using immunofluorescence microscopy. Images of hematoxylin and eosin (HE) and immunohistochemistry (IHC) staining were captured using a Leica DM750 microscope equipped with EC3 digital camera and LAS EZ software. The magnification time was two hundred. The image of IF was obtained with a ZEISS IF microscope and AxioVision Rel. 4.8 software. The magnification time was four hundred. At least 5 areas were randomly selected from each sample using ImageJ 1.52 software. They were quantified. The slides were disposed with standard cell regulator 1 for sixty minutes. The primary antibody as anti-ki67 (1:100, Abcam) was added in. They were incubated at 37 °C for 1 hour. Secondary antibody staining was performed. Sections were counterstained with hematoxylin for 4 minutes, followed by bluing in ammonia water for 4 minutes (Magaki *et al*., 2019).

Immunofluorescence staining

The relevant steps of immunofluorescence staining were completed according to the operation methods in previous literature (Donaldson., 2015). Cells in the miRNA/siRNA-treated group and the negative control (NC) group were seeded in 6-well plates. Cells were fixed 48 hours post-transfection for immunofluorescence staining. Four hundred microliters of DMF was added in. 40 mg of the colorful developing agent was dissolved in 2 mL of PBS. The substrate solution was mixed with developing solution. They were added in ells. They were incubated at 37 °C for 30 minutes. They were observed under microscope.

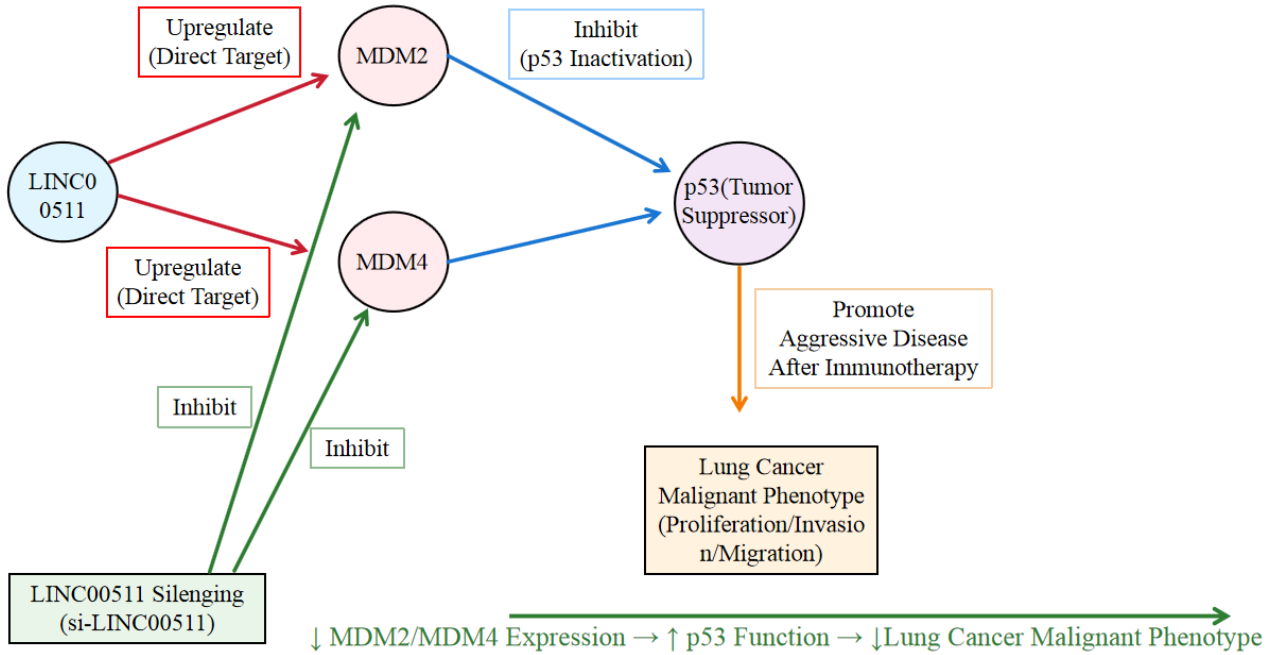

Fig. 1: Schematic diagram of the signal pathway mechanism

Establishment of mouse xenograft model

Six-week-old female BALB/c nude mice weighing 18 – 22 g (mean ± SD: 20.1 ± 1.2 g) were purchased from the animal experiment center of the institute. For in vivo experiments, each group contained 6 mice (n = 6 per group). The experimental unit was a single mouse. Mice were housed in individually ventilated cages (IVCs) with autoclaved bedding, nesting material (e.g., cotton squares) and a plastic tunnel for environmental enrichment. Cage enrichment was provided to reduce stress and standardize behavioral conditions. They were housed under specific pathogen-free conditions at 22 ± 2°C, with free access to food and water and a 12:12 light: dark cycle. Animals were allowed to acclimate to the housing environment for 7 days prior to any experimental procedures. Exclusion criteria established a priori were: failure of tumor engraftment by day 7, signs of illness (e.g., lethargy, hunched posture), or weight loss >15%. No animals met these criteria. Mice were randomly assigned to experimental or control groups using a computer-generated random number sequence. To minimize confounding, treatment order was randomized across groups and cage positions were balanced in the housing rack. The nude mouse xenograft model was established using methods described in previous studies (Zhang *et al*., 2025). Briefly, after infecting A549 cells with shRNA lentivirus, 4×10^6 cells were suspended in 100 µL PBS and subcutaneously injected into the right flank based on preliminary dose-response experiments and previous studies (Zhang *et al*., 2025) of six-week-old female BALB/c nude mice under isoflurane inhalation anesthesia.Post-operatively, all mice received buprenorphine (0.05-0.1 mg/kg subcutaneously) every 8 – 12 hours for 48 hours to alleviate pain. No additional analgesia was required. The animal experimental protocol for this study was approved by the animal ethics committee of the institute (Approval number: FLPH-2021-008). Tumor volume was measured every other day to capture dynamic changes in tumor growth while minimizing animal handling stress, consistent with standard practice in xenograft studies (Zhang *et al*., 2025). Humane endpoints: Mice were monitored daily for clinical signs. The following humane endpoints were established a priori and approved by the ethics committee: tumor volume exceeding 1500 mm^3 , weight loss >20% of initial body weight, inability to access food/water, persistent lethargy, or tumor ulceration. Any mouse reaching these endpoints was immediately euthanized. No mouse reached these endpoints during the study. The tumor was collected and weighted after the experiment was terminated. And they were pictured. Mice in the experimental group were intraperitoneally injected with the PD-1 inhibitor Nivolumab (0.1 mg/kg) every three days, while the control group was injected with an equal volume of PBS ; this dose was selected based on published protocols in similar xenograft models (Chiang *et al*., 2023) and preliminary dose-finding studies showing efficacy without overt toxicity. The control group received an equal volume of PBS via intraperitoneal injection every three days under the same schedule. Tumor size was monitored by imaging. It in mice with aggressive disease was compared with mice with tumor extinction. Outcome assessments, including tumor volume measurement, immunohistochemistry scoring and cell counting, were performed by investigators blinded to group allocation.

Western blot assay

Western Blot analysis was performed following the method described in previous studies (Pillai-Kastoori *et al*., 2020). The procedure was briefly as follows: After lysis with cell lysis buffer, the samples were incubated overnight at 4°C with primary antibodies against MDM2 (1:1000, CST #86934) and MDM4 (1:1000, Abcam ab134153). GAPDH (CST #5174) was used as an internal control. Protein bands were analyzed using the ChemiDoc imaging system (Bio-Rad). Each independent experiment was performed with three biological replicates per condition and the experiment was repeated three times (n = 3 per group). The experimental unit was one protein lysate sample from an independent well.

RT-PCR

RNA extraction and RT-PCR were performed according to the manufacturer's instructions (Thermo Fisher, Shanghai, Cat. No. AQ601-01) and the procedure described by Moufarrej *et al*. (Moufarrej and Quake., 2023). The TM microRNA qPCR quantitative kit was adopted. The U6 expression was set as endogenous control.The primer sequences were as follows: LINC00511 forward 5'-TGGCTTGTCTTCCATCGTCC-3', reverse 5'-GCACGAGGGTTGTTACAGGA-3'; MDM2 forward 5'-TTGGCGTGCCAAGCTTCTCT-3', reverse 5'-TACCTGAGTCCGATGATTCC-3'; U6 forward 5'-CTCGCTTCGGCAGCACA-3', reverse 5'-AACGCTTCACGAATTTGCGT-3'. Each independent experiment was performed in triplicate wells per condition and the experiment was repeated three times (n = 3 per group). The experimental unit was one well.

Cell migration and invasion test

A Transwell pad with a 0.8 μm polycarbonate filter was used for analysis of Transwell migration. After transfection, 5×10^4 cells were seeded into the upper chamber of a Transwell (8 μm polycarbonate membrane). The Transwell membrane was added into upper chamber. The exosome suspended in complete medium (containing 5×10^4 cells) was added into lower chamber. Incubate at 37°C for 24 hours to allow the cells to penetrate the membrane. Cell migration and invasion were assessed at 24 hours post-transfection. The migrated cells were fixed with four percent of formalin. They were dyed. Cellular morphology was observed under a microscope. Ten random areas were collected to quantify the migration. Each independent experiment was performed in triplicate wells per condition and the experiment was repeated three times. The experimental unit was one well.

The invasion assay was performed in Transwell chambers precoated with 1 mg/mL Matrigel, with 1×10^5 cells seeded in each well (Marshall J., 2011). Complete medium was added to each well. They were cultivated for twenty-four hours. The non-invasive cells were removed with cotton swab. The migrated cells were fixed with 4% formalin. They were dyed. Cellular morphology was observed under a a microscope. Cells that migrated to the lower surface of the membrane were collected. The quantity of invasion was counted. Each independent experiment was performed in triplicate wells per condition and the experiment was repeated three times (n = 3 per condition). The experimental unit was one well.

Cell proliferation assay

Cell proliferation was assessed using the CCK-8 assay (Dojindo, Japan) at 0, 24, 48 and 72 hours post-transfection, according to the manufacturer's instructions. Each experiment was performed in triplicate wells and repeated three times independently (n = 3 per time point).

Outcome measures

The primary outcome was tumor volume change over time. Secondary outcomes included migration, invasion, proliferation (Ki-67) and expression levels of LINC00511, MDM2 and MDM4.

Adverse events

Mice were monitored daily for signs of distress, wound infection, or abnormal behavior. No adverse events were observed during the study period.

Statistical analysis

The SPSS22.0 software and Graphad Prism 6 software was adopted. Continuous data are presented as mean ± standard deviation (SD). Student’s t-test was used for comparisons between two groups. Normality of data was assessed using the Shapiro‑Wilk test. Homogeneity of variances was checked using Levene's test. When assumptions were violated, non-parametric tests (Mann-Whitney U) were applied. There was significant difference ($P < 0.05$). Sample sizes for animal experiments were determined based on a power analysis assuming an effect size of 1.5, $\alpha = 0.05$ and power = 0.80, yielding a minimum of 5 mice per group. To account for potential dropouts, 6 mice per group were used. For in vitro experiments, a minimum of three independent replicates (n = 3) were performed based on standard practice in the field.

RESULTS

Expression of LINC00511 and MDM2/MDM4 in lung carcinoma with aggressive disease after immunotherapy

No animals or samples were excluded from the analysis. All randomized animals were included in the final analysis. LINC00511 expression was significantly elevated in lung carcinoma tissues (5.34 ± 0.45 vs. 2.16± 0.22; 95% CI for difference: 1.08 to 1.60, P < 0.01) (Fig. 2A). There was notable positive correlation between staging of lung carcinoma and LINC00511 expression (Fig. 2B). There was high expression of MDM2/MDM4 in tumor tissue (Fig. 2C).

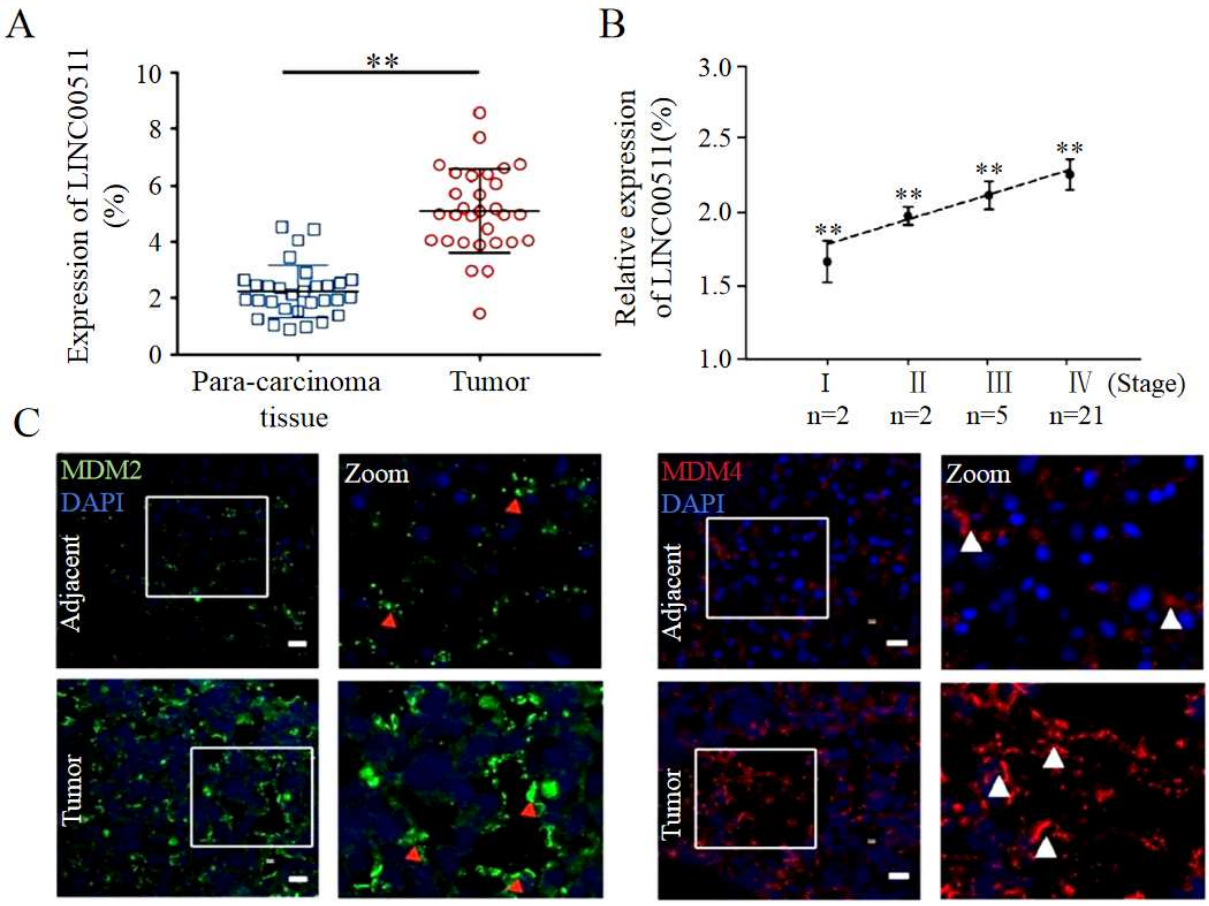

Fig. 2: Expression of LINC00511 and MDM2/MDM4 in immunological therapy for lung carcinoma with aggressive disease.
(A) LINC00511 expression detected with RT-PCR; (B) LINC00511 expression in different staging; (C) Expression of MDM2/MDM4 in tumor tissue detected with IF method. **represented as $P < 0.01$. The proportion of IF was one to two hundred.

LINC00511 targets and regulates the expression of MDM2/MDM4

The binding site between LINC00511 and MDM2/MDM4 was predicted using the StarBase online detection tool. LINC00511 directly targets MDM2/MDM4, as confirmed by luciferase reporter assays (Figs. 3A and 3B). The luciferase activity in the wild-type set could be reduced. However, luciferase activity in the MDM2/MDM4-Mut set was not affected (Figs. 3C and 3D). The LINC00511 expression could be increased if the expression of MDM2/MDM4 was reduced (Fig. 3E). There was targeting regulatory effect between LINC00511 and MDM2/MDM4.

Biological functions of lung carcinoma cells could be induce with MDM2/MDM4

Knockdown of MDM2/MDM4 significantly reduced the invasive and migratory capabilities of A549 cells (Fig. 4A). The expression of N-cadherin, Slug and Twist could be reduced notably if there was low expression of MDM2/MDM4. But expression of E-cadherin could be increased (Fig. 4B). So cell migration could be retarded by MDM2/MDM4 through inducing the EMT transition. The proliferative activity could be reduced notably, along with a reduction in MDM2/MDM4 expression (Figs. 4C and 4D).

Intervention in LINC00511 expression reverses the progression of lung cancer

The gross tumor volume could be reduced in test set (si-LINC00511: 445.6 ± 45.3 vs. control 720.4 ± 80.2 ; 95% CI: 410.2-481.0 mm^3 vs. 660.5-840.3 mm^3; $P < 0.01$, Cohen's d = 3.2). The growth of tumor cells could be notably restrained by the administration of si-LINC00511 (Figs. 5A and 5B). The quantity of proliferated ki76 cells could also be reduced notably with the disposal of si-LINC00511 (Fig. 5C).

DISCUSSION

Immunotherapy plays a crucial role in modulating the tumor microenvironment, supported by continuous advancements in fundamental research. Immune-targeting drugs have been progressively developed.

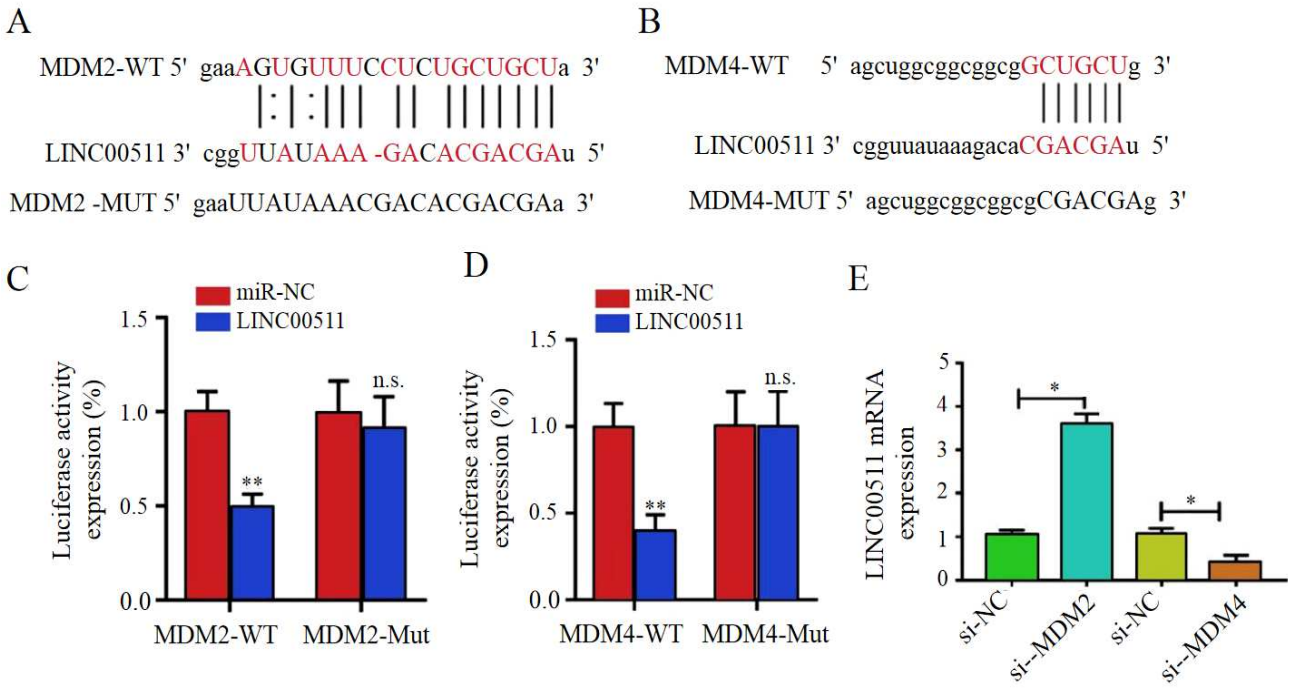

Fig. 3: LINC00511 could be targeting the expression of MDM2/MDM4 in lung carcinoma cells
(A) Expression of LINC00511 and MDM2 detected with bioinformatics; (B) Expression of LINC00511 and MDM4; (C and D) Analysis on the luciferase activity; (E) LINC00511 expression detected with RT-PCR
* represented as $P < 0.05$. ** represented as $P < 0.01$.

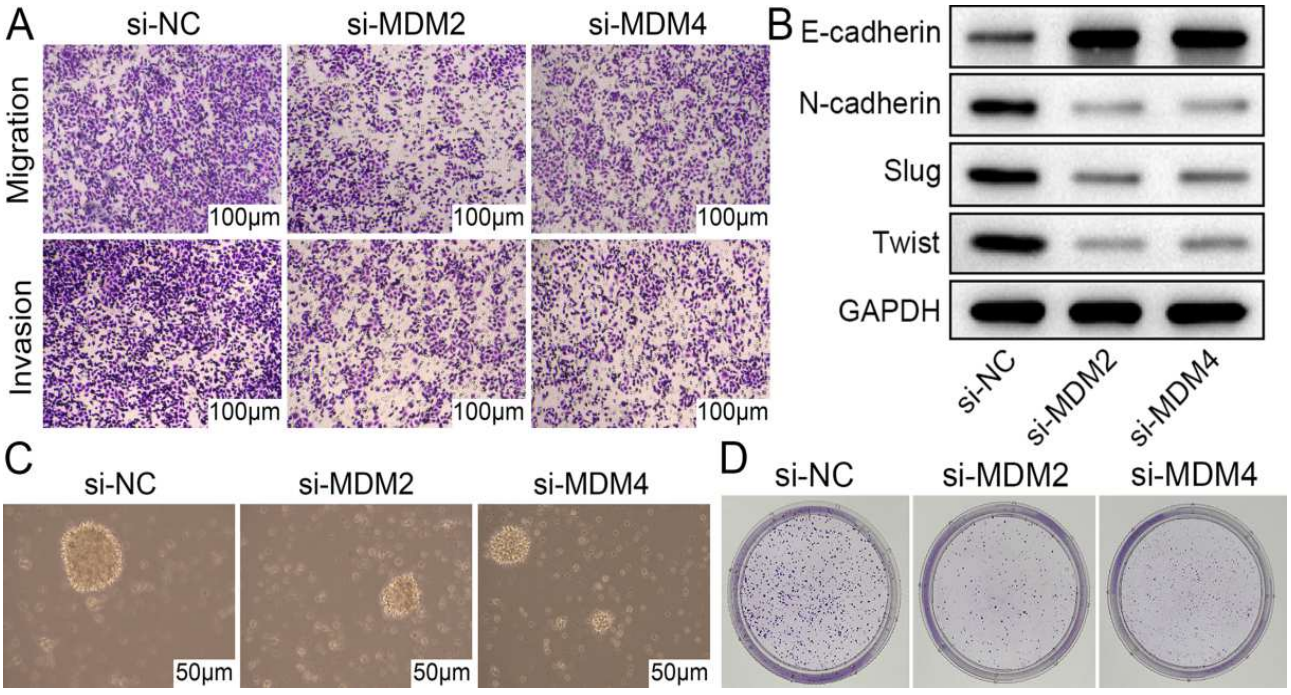

Fig. 4: Biological functions of lung carcinoma cells could be induce with MDM2/MDM4
(A) Cell migration detected with Transwell; (B) Expression of related protein detected with Western Blot assay. The number represented as gray value in detected related expression quantity of protein; (C) Proliferative ability detected with balling test; (D) Proliferative expression detected with cell cloning test. The proportion was one to two hundred.

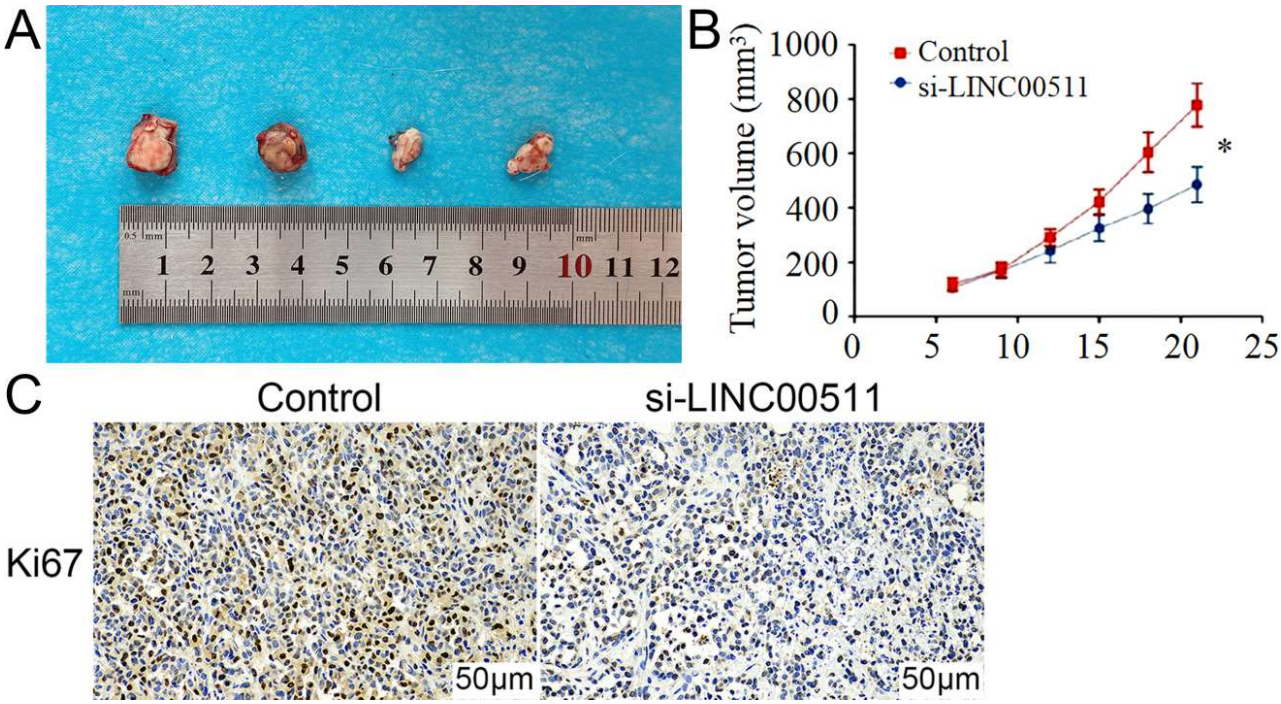

Fig. 5: Development of lung carcinoma could be reversed rapidly with intervening the LINC00511 expression
(A) General figure of tumor; (B) Tumor volume; (C) Ki67 expression detected with IHC. * represented as $P < 0.01$. The proportion was one to one hundred.

Although immunotherapy shows clinical efficacy, the overall response rate remains limited. Approximately 20–30% of patients experience varying degrees of disease progression during treatment (Zhang *et al*., 2023). A subset of patients exhibits slow disease progression. It was called as pseudoprogression. This led to the establishment of the iRECIST criteria for evaluating immunotherapy responses. Aggressive disease is not specific to immunotherapy. Aggressive disease has also been reported in chemotherapy and targeted therapy (Lennartz *et al*., 2020, Qiao *et al*., 2025).

The mechanisms underlying aggressive disease are multifactorial. The tumor microenvironment can be altered by various factors, including decreased antigen presentation and infiltration of immunosuppressive cells such as myeloid-derived suppressor cells and regulatory T cells (Tregs) (Khalaf *et al*., 2021, Qian *et al*., 2025). The findings suggest that LINC00511 promotes aggressive lung cancer by directly regulating MDM2/MDM4 expression. LINC00511 influences tumorigenesis and progression by activating downstream signaling pathways (Song *et al.,* 2023).

The reported incidence of aggressive disease varies considerably across studies, which may be attributed to differences in tumor types, definitions of aggressive disease and small sample sizes (e.g., n = 30 in the clinical tissue cohort). Several limitations should be noted. First, the use of the A549 human lung adenocarcinoma cell line and the BALB/c nude mouse xenograft model provides preliminary mechanistic evidence but lacks a fully functional immune system, limiting the generalizability of the findings to immunocompetent settings or other lung cancer subtypes. Second, although outcome assessors were blinded to group allocation as stated in Methods, the possibility of residual detection bias cannot be completely excluded and this represents a study limitation. Third, no confidence intervals were reported for effect estimates, limiting the precision assessment of the results. Clinical validation in larger, well-defined patient cohorts is therefore required. The survival prognosis of patients with aggressive disease was notably worse. The median OS in patients with aggressive disease was 3.4 months. And the central OS in patients without AD was 6.2 months (P=0.003). However, no survival difference was observed between AD and non-AD patients in a chemotherapy subgroup (n = 59), likely due to the small sample size (Guiard *et al*., 2022). There was difference in survival prognosis in normal PD and AD through treatment of signal drug in immunological therapy. There were fifty cases of AD in ninety-nine cases of PD patients. The central OS for PD patients was 205 days. The central OS of AD patients was only fifty days (HR, 5.079; 95% CI, 3.138-8.226). Similar results were reported (Lin *et al*., 2021, Zhang *et al*., 2021). Immune checkpoint inhibitors can enhance IFN-γ expression. The expression of IRF-8 could be induced and the downstream JAK-STAT signaling

pathway could be activated. The expression of MDM2 could be induced by combining the MDM2 promoter (Han et al., 2023; Su *et al*., 2025). This cascade response is less pronounced in the absence of MDM2 amplification. The AD could be caused if MDM2 was amplified. Other hypotheses have also been proposed (Sun *et al*., 2024; Zang *et al*., 2020). PD-1 blockade enhances T-cell activity and $CD8^+$ T-cell cytotoxicity. The therapeutic effect could be enhanced further. However, only a subset of patients responds favorably to immunotherapy, often due to an immunosuppressive tumor microenvironment. The amplification of MDM2 was considered a potential mechanism underlying rapid tumor growth in some patients after immunotherapy (Sun *et al*., 2024). The phase I study on MDM2 was being developed to prevent the occurrence of AD (Adashek *et al*., 2020). The aggressive nature of lung carcinoma could be caused by abnormal MDM2/MDM4 expression.

CONCLUSION

This study demonstrates that LINC00511 is significantly upregulated in lung carcinoma tissues from patients with aggressive disease following immunotherapy and its expression level correlates positively with tumor stage. Mechanistically, LINC00511 directly binds to and upregulates MDM2/MDM4 expression, thereby enhancing tumor cell proliferation, migration, invasion and epithelial-mesenchymal transition. Knockdown of LINC00511 effectively suppresses these malignant phenotypes in vitro and significantly reduces xenograft tumor growth in vivo. These findings suggest that LINC00511 may serve as a potential predictive biomarker for identifying patients at risk of aggressive disease during immunotherapy and that targeting the LINC00511/MDM2/MDM4 axis could represent a novel therapeutic strategy. However, the use of immunodeficient BALB/c nude mice limits the ability to fully assess the interplay between LINC00511 and the adaptive immune response and the relatively small clinical sample size (n = 30) warrants cautious interpretation. Future studies should validate these findings in immunocompetent animal models and larger patient cohorts and investigate whether combining LINC00511 inhibition with immune checkpoint blockade produces synergistic antitumor efficacy.

Acknowledgments
The authors thank the laboratory staff at the Fourth Medical Center of the PLA General Hospital for their technical support.

Author's contributions
Qiuwen Li: Conceptualization, Methodology, Software, Formal Analysis and Writing - review & editing;
Fengyun Zhang: Investigation, Data Curation, Project administration, Writing - Original Draft;

Funding
This research received no specific grant from any funding agency in the public, commercial, or not-for-profit sectors.

Data availability statement
The data supporting the findings of this study are available from the corresponding author upon reasonable request.

Ethical approval
All tissue samples were obtained with written informed consent from the patients and the study protocol was approved by Ethics Committee of the Fourth Medical Center of the PLA General Hospital **(**Approval number: FLPH-2021-008). A study protocol for the animal experiments was prepared prior to the study and is available from the corresponding author upon reasonable request. This animal study was conducted in compliance with the ARRIVE guidelines.

Conflict of interest
The author states that this research was conducted without any commercial or financial interests that could be interpreted as potential conflicts of interest. There are no conflicts to declare.

Supplementary data
https://www.pjps.pk/uploads/2026/07/SUP1784796700.pdf

REFERENCES

Abdi E, Latifi-Navid S, Panahi A and Latifi-Navid H (2023). LncRNA polymorphisms and lung cancer risk. *Per Med*., **20**(6): 511–522.

Adashek JJ, Subbiah IM, Matos I, Garralda E, Menta AK, Ganeshan DM and Subbiah V (2020). Hyperprogression and immunotherapy: Fact, fiction, or alternative fact. *Trends Cancer*., **6**(3): 181–191.

Chiang CY, Huang MC, Tsai SC, Hsu FT, Liao TL, Yu JH, Lin TH, Huang HH and Liao PA (2023). Humanized PD-1 knock-in mice reveal nivolumab's inhibitory effects on glioblastoma tumor progression *in-vivo*. *In-vivo*., **37**(5): 1991–2000.

Deng H, Gao X, Peng H, Wang J, Hou X, Xu H and Yang F (2018). Effect of liposome–mediated HSP27 transfection on collagen synthesis in alveolar type II epithelial cells. *Mol Med Rep*., **17**(5), 7319–7324.

Donaldson JG (2015). Immunofluorescence Staining. *Curr Protoc Cell Biol*., **69**, 431–437.

Gao W, Huang J, Deng K, Lin X, Long X, Li X, Huang M, Wang X, She X, Liu Q and Wu M (2026). Endothelial cells sense temozolomide resistance to facilitate monocyte-derived macrophage infiltration in glioblastoma. *Drug Resist Updat*., **84**: 101329.

Guiard E, Baldini C, Pobel C, Assi T, Bernard-Tessier A, Martin-Romano P, Hollebecque A, Verlingue L, Geraud

A, Michot JM, Armand JP, Soria JC, Massard C and Ammari S (2022). Radiological patterns of tumour progression in patients treated with a combination of immune checkpoint blockers and antiangiogenic drugs. *Eur J Cancer*., **167**: 42–53.

Han J, Wu M and Liu Z (2023). Dysregulation in IFN-γ signaling and response: The barricade to tumor immunotherapy. *Front Immunol*., **14**: 1190333.

Hu WY, Wei HY, Li KM, Wang RB, Xu XQ and Feng R (2020). LINC00511 acts as a ceRNA, promoting malignant cell behaviors and correlating with the prognosis of hepatocellular carcinoma patients by modulating the miR-195/EYA1 axis. *Biomed Pharmacother*., **121**: 109642.

Ippolito D, Maino C, Ragusi M, Porta M, Gandola D, Franzesi CT, Giandola TP and Sironi S (2021). Immune response evaluation criteria in solid tumors for assessment of atypical responses after immunotherapy. *World J Clin Oncol*., **12**(5): 323–334.

Kai-Xin L, Cheng C, Rui L, Zheng-Wei S, Wen-Wen T and Peng X (2021). Roles of lncRNA MAGI2-AS3 in human cancers. *Biomed Pharmacother*., **141**: 111812.

Khalaf K, Hana D, Chou JT, Singh C, Mackiewicz A and Kaczmarek M (2021). Aspects of the tumor microenvironment involved in immune resistance and drug resistance. *Front Immunol*., **12**: 656364.

Koelsche C, Benhamida JK, Kommoss FKF, Stichel D, Jones DTW, Pfister SM, Heilig CE, Frohling S, Stenzinger A, Buslei R, Mentzel T, Baumhoer D, Ladanyi M, Antonescu CR, Flucke U, Gorp JV, Bode-Lesniewska B, Deimling AV and Mechtersheimer G (2021). Intimal sarcomas and undifferentiated cardiac sarcomas carry mutually exclusive MDM2, MDM4 and CDK6 amplifications and share a common DNA methylation signature. *Mod Pathol*., **34**(12): 2122–2129.

Lennartz S, Diederich S, Doehn C, Gebauer B, Grünwald V, Notohamiprodjo M, Sommer W, Schlemmer HP and Persigehl T (2020). Radiological monitoring of modern immunotherapy: A novel challenge for interdisciplinary patient care. radiologisches monitoring von modernen immuntherapien: Neue herausforderung fur die interdisziplinare zusammenarbeit. *Rofo*., **192**(3): 235–245.

Lin M, Vanneste BGL, Yu Q, Chen Z, Peng J and Cai X (2021). Hyperprogression under immunotherapy: A new form of immunotherapy response?-a narrative literature review. *Transl Lung Cancer Res*., **10**(7): 3276–3291.

Liu B, Zhou F, Liu H, Wang Y, Wang J, Ren F and Xu S (2022). Knockdown of LINC00511 decreased cisplatin resistance in non-small cell lung cancer by elevating miR-625 level to suppress the expression of leucine rich repeat containing eight volume-regulated anion channel subunit E. *Hum Exp Toxicol*., **41**: 9603271221089000.

Liu J, Yang J, Pan Q, Wang X, Wang X, Chen H, Zheng X and Huang Q (2024). MDM4 was associated with poor prognosis and tumor-immune infiltration of cancers. *Eur J Med Res*., **29**(1): 79.

Magaki S, Hojat SA, Wei B, So A and Yong WH (2019). An introduction to the performance of immunohistochemistry. *Methods Mol Biol*., **1897**: 289–298.

Marshall J (2011). Transwell(®) invasion assays. *Methods Mol Biol*., **769**: 97–110.

Moufarrej MN and Quake SR (2023). An inexpensive semi-automated sample processing pipeline for cell-free RNA extraction. *Nat Protoc*., **18**(9): 2772–2793.

Nuñez NG, Berner F, Friebel E, Unger S, Wyss N, Gomez JM, Purde MT, Niederer R, Porsch M, Lichtensteiger C, Kramer R, Erdmann M, Schmitt C, Heinzerling L, Abdou MT, Karbach J, Schadendorf D, Zimmer L, Ugurel S, Klümper N and Flatz L (2023). Immune signatures predict development of autoimmune toxicity in patients with cancer treated with immune checkpoint inhibitors. *Med*., **4**(2): 113–129.e7.

Pillai-Kastoori L, Schutz-Geschwender AR and Harford JA (2020). A systematic approach to quantitative Western blot analysis. *Anal Biochem*., **593**: 113608.

Qian X, Yi W, Yan W, Cai Y, Hu S, Yan D, Zhao Z, Li R, Wang L, Xu H and Li Y (2025). Cryo-shocked tumor-reprogrammed sonosensitive antigen-presenting cells improving sonoimmunotherapy via T cells and NK cells immunity. *Adv Mater*., **37**(12): e2413289.

Qiao T, Cheng Z and Duan Y (2025). Innovative applications and future trends of multiparametric PET in the assessment of immunotherapy efficacy. *Front Oncol*., **14**: 1530507.

Reck M, Dziadziuszko R, Sugawara S, Kao S, Hochmair M, Huemer F, de Castro G, Jr Havel L, Bernabe Caro R, Losonczy G, Lee JS, Kowalski D M andric Z, Califano R, Veatch A, Gerstner G, Batus M, Morris S, Kaul M, Cuchelkar V and Liu SV (2024). Five-year survival in patients with extensive-stage small cell lung cancer treated with atezolizumab in the Phase III IMpower133 study and the Phase III IMbrella A extension study. *Lung Cancer*., **196**: 107924.

Rodrigo JP, Moreno-Bueno G, Lequerica-Fernandez P, Rodriguez-Santamarta T, Diaz E, Prieto-Fernandez L, Alvarez-Teijeiro S, Garcia-Pedrero JM and de Vicente JC (2024). Tumor-intrinsic perinuclear LOXL2: prognostic relevance and relationship with YAP1 activation status in oral squamous cell carcinoma. *Pathobiology*, **91**(6): 422–433.

Siegel RL, Kratzer TB, Giaquinto AN, Sung H and Jemal A (2025). Cancer statistics, 2025. *CA Cancer J Clin*., **75**(1): 10–45.

Song Z, Luo J, Wu M and Zhang Z (2023). linc00511 knockdown inhibits lung cancer progression by regulating miR-16-5p/MMP11. *Crit Rev Eukaryot Gene Expr*., **33**(7): 17–30.

Su Z, Ding Y, Xue J, Sun J and Ji C (2025). Identifying SUMOylation-related genes in liver fibrosis with bioinformatics and experimental models for diagnostic insights. *Sci Rep*., **15**(1): 39783.

Sun D, Qian H, Li J and Xing P (2024). Targeting MDM2

in malignancies is a promising strategy for overcoming resistance to anticancer immunotherapy. *J Biomed Sci*., **31**(1): 17.

Wu Y, Guo X, Jin L, Huang G, Niu L and Zhao Y (2024). Lnc-LINC00511 promotes gastric cancer progression by regulating MiR-29c-3p/TRIP13 axis through AKT/mTOR pathway. *Int J Biol Macromol*., **281**: 136455.

Zang H, Peng J, Zheng H and Fan S (2020). Hyperprogression after immune-checkpoint inhibitor treatment: Characteristics and hypotheses. *Front Oncol*., **10**: 515.

Zhang H, Fang X, Li D, Yang M, Yu L, Ding Y, Shen H and Yuan Y (2021). Hyperprogressive disease in patients receiving immune checkpoint inhibitors. *Curr Probl Cancer*., **45**(3): 100688.

Zhang H, Yue X, Chen Z, Liu C, Wu W, Zhang N, Liu Z, Yang L, Jiang Q, Cheng Q, Luo P and Liu G (2023). Define cancer-associated fibroblasts (CAFs) in the tumor microenvironment: New opportunities in cancer immunotherapy and advances in clinical trials. *Mol Cancer*., **22**(1): 159.

Zhang Y, Tang Z, Zhao W, Chu Y, Chen J and Chen D (2025). Attenuated Salmonella typhimurium L forms combined with lentivirus shRNA-HOTAIR effectively inhibit tumor growth and metastasis in murine epithelial ovarian cancer. *Eur J Pharmacol*., **1005**: 178109.

Zhang Y, Xiao P and Hu X (2022). LINC00511 enhances LUAD malignancy by upregulating GCNT3 via miR-195-5p. *BMC Cancer*., **22**(1): 389.